Chemical and Physical Studies on the Reaction Mechanism of Charge-Transfer Complexes Between Narcotic Drugs and Electronic Acceptors

Abdel Majid A. Adam[1], Mahmoud Salman[2], T. Sharshar[3,4], Moamen S. Refat[1,5]*

[1] Department of Chemistry, Faculty of Science, Taif University, Al-Haweiah, P.O. Box 888, Zip Code 21974, Taif, Saudi Arabia
[2] Al-Hussein Bin Talal University, P.O. Box 20 Ma'an, Jordan
[3] Department of Physics, Faculty of Science, Taif University, Al-Haweiah, P.O. Box 888, Zip Code 21974, Taif, Saudi Arabia
[4] Department of Physics, Faculty of Science, Kafrelsheikh University, Kafr El-Sheikh, Egypt
[5] Department of Chemistry, Faculty of Science, Port Said University, Port Said, Egypt
[*]E-mail: majidadam@yahoo.com

Considerable attention has recently been devoted to the formation of stable charge-transfer complexes that result from the reaction between acceptors and drugs. This interest stems from the significant physical and chemical properties of these complexes. In this paper, the charge-transfer complexes formed between the ephedrine (Eph) drug as a donor with picric acid (Pi) and quinol (QL) as a π–acceptors have been synthesized in methanol as a solvent at room temperature and spectroscopically studied. Based on the elemental analyses (C, H and N) and photometric titrations, the interaction between both picric and quinol π–acceptors with Eph donor formed via a stoichiometry (drug: acceptors) of 1:2 and 1:1, respectively. Benesi-Hildebrand and its modification methods were applied to estimate the spectroscopic and physical data. The spectroscopic techniques such as (infrared, ^{1}H-NMR, and UV-vis) spectra, positron annihilation lifetime and thermo gravimetric analysis (TG) were used to characterize the chelating behavior of the synthetic CT complexes. The positron annihilation lifetime parameters were found to be dependent on the structure, electronic configuration and molecular weight of CT complexes. Finally, the antimicrobial activity of the CT complexes was determined against various bacterial and fungal strains.

1. INTRODUCTION

Charge–transfer (CT) complexation is currently achieve the great importance in biochemical, bioelectrochemical energy transfer process [1], biological systems [2], and drug-receptor binding mechanism, for examples, drug action, enzyme catalysis, ion transfers through lipophilic membranes [3], and certain π-acceptors have successfully been utilized in pharmaceutical analysis of some drugs in pure form or in pharmaceutical preparations [4-10]. Recently, many studies have been widely reported about the rapid interactions between different kinds of drugs and related compounds as donors like morpholine, norfloxacin, ciprofloxacin, and sulfadoxine, with several types of σ and π-electron acceptors [11-25]. Various spectroscopic techniques were used to characterize different types of complexes. Recently, positron annihilation spectroscopy is also applied to CT complexes [26-29]. Positron annihilation lifetime (PAL) spectroscopy is one of the highly successful techniques, which have been used to study the structural aspects of different types of materials even at subatomic levels. When a positron is emitted from a ^{22}Na source and allowed to penetrate the materials, it thermalizes and diffuses to a depth of a few hundred μm. The positron either delocalizes or traps in defects, which lead to an increase of its lifetime, or extracts an electron from the surrounding material to form a positronium atom (Ps) with two states, a singlet state (para-Ps, p-Ps) and a triplet state (ortho-Ps, *o*-Ps). In both cases, the positron will eventually annihilate with an electron and will have a corresponding lifetime for each state at annihilation site. Each lifetime component has a corresponding intensity (I_i) relating to the number of annihilations occurring at a particular lifetime (τ_i). The measured parameters of the Ps formation in ionic and molecular solids (τ and I) depend on the physical and chemical properties of the solids [30, 31]. The previous studies show that the Ps is preferentially formed in compounds exhibiting negative charge stabilization at specific sites. These studies also show that the parameters of positron annihilation are sensitive to the liability of the solids to charge-transfer processes and it mainly dependent on the nature of the central of acceptor [27, 29]. Also, the correlation between positron annihilation parameters and the structure of the CT complexes was observed [27, 29].

Herein, the CT interaction between the two π–acceptors (picric acid and quinol) with one of narcotic drug like ephedrine was investigated. The nature and structure of the final products have been characterized to interpret the behavior of interactions using elemental analysis, infrared (IR), ^{1}H-NMR, electronic spectra and positron annihilation lifetime spectra. The spectroscopic and physical data were analyzed in terms of formation constant (K_{CT}), molar extinction coefficient (ε_{CT}), standard free energy ($\Delta G°$), oscillator strength (f), transition dipole moment (μ), resonance energy (R_N) and ionization potential (I_D). Finally, the antimicrobial activity of the CT complexes was determined against various bacterial and fungal strains.

2. EXPERIMENTAL METHODS

2.1 Chemicals

All chemical used were of high grade. The ephedrine (MF= $C_{10}H_{15}NO$) were obtained from Sigma-Aldrich Chemical Company, USA and were used without further purification. Picric acid

(2,4,6-trinitro-1-phenol; Pi) and quinol (benzene-1,4-diol; QL) was purchased from Merck Chemical Company and were also used as received.

2.2 Reaction Procedure

The solid CT products of Eph with Pi and QL were synthesized by mixing equimolar amounts of Eph drug with Pi and QL acceptors in methanol. The mixtures were stirred for 20 min, and allowed to evaporate slowly at room temperature, which resulted in the precipitation of the solid CT complexes. The separated complexes were filtered off, washed well with little amounts of methanol, and then collected and dried under vacuum over anhydrous calcium chloride for 24 h.

2.3 Photometric titration

Photometric titration measurements were carried out for the reactions of Eph with Pi and QL against methanol as a blank at wavelengths of 393 and 294 nm, respectively. A= 0.25, 0.50, 0.75, 1.00, 1.50, 2.0, 2.50, 3.00, 3.50 or 4.00 ml aliquot of a standard solution (5.0×10^{-4} M) of the Pi or QL acceptor in MeOH was added to 1.00 ml (5.0×10^{-4} M) of Eph drug, which was also dissolved in MeOH. The total volume of the mixture was 5 ml. The concentration of the donors (C_d) in the reaction mixture was maintained at 5.0×10^{-4} M, whereas the concentration of the respective acceptor (C_a) changed over a wide range of concentrations (0.25×10^{-4} M to 4.00×10^{-4} M) to produce solutions with molar ratio varied from 4:1 to 1:4. The stoichiometry of the molecular CT complexes was obtained from the determination of the conventional spectrophotometric molar ratio according to known methods [32] using a plot of the absorbance of each CT complex as a function of the C_d:C_a ratio. Modified Benesi–Hildebrand plots [33, 34] were constructed to allow the calculation of the formation constant, K_{CT}, and the absorptivity, ε_{CT}, values for each CT complex in this study.

2.4 Instrumentation

The elemental analyses of the carbon, hydrogen and nitrogen contents were performed using a Perkin-Elmer CHN 2400 (USA). The electronic absorption spectra of methanolic solutions of the donor, acceptors and resulting CT complexes were recorded over a wavelength range of 200-800 nm using a Perkin-Elmer Lambda 25 UV/Vis double-beam spectrophotometer. The instrument was equipped with a quartz cell with a 1.0 cm path length. The mid-infrared (IR) spectra (KBr discs) within the range of 4000-400 cm^{-1} for the solid CT complexes were recorded on a Shimadzu FT-IR spectrophotometer with 30 scans at 2 cm^{-1} resolution. ^{1}H-NMR spectra were collected by a Bruker DRX-250 spectrometer operating at 250 MHz with a dual 5 mm probe head. The measurements were performed at ambient temperature using DMSO-d_6 (dimethylsulfoxide, d_6) as a solvent and TMS (tetramethylsilane) as an internal reference. The ^{1}H-NMR data are expressed in parts per million (ppm) and are internally referenced to the residual proton impurity in the DMSO solvent. Thermogravimetric

analysis (TG) was performed under static air atmosphere between room temperature and 800 °C at a heating rate of 10 °C/min using a Shimadzu TGA–50H thermal analyzer.

The PAL measurements were carried out using a fast-fast coincidence spectrometer [35]. This PAL spectrometer consists of two Bicron BC-418 plastic scintillation detectors and Ortec modules; two 583 constant fraction differential discriminators (CFDD), DB643 delay box (ns D), 414A fast coincidence and 566 time-to-amplitude converter (TAC). The data were acquired using an Ortec 919 multichannel analyzer (MCA). A positron source was prepared using a droplet of ^{22}NaCl solution dried onto two identical Kapton foils (7.5 μm thick), which were afterward glued by epoxy glue. This source was sandwiched between two identical samples. The lifetime spectra were measured in air at room temperature. More than one million counts were accumulated for each spectrum and each sample was measured three times. The time resolution of the spectrometer, measured with ^{60}Co source at ^{22}Na energy window settings, was ~300 ps (full-width at half maximum). The positron annihilation lifetime is measured experimentally as the time interval between the 1274.5 keV γ ray emitted by the ^{22}Na radioisotope and one of the annihilation radiations. The resulting lifetime spectra were analyzed using a computer program LT [36] with a suitable correction for positrons annihilated in the Kapton. The lifetime spectra decomposed into two and three components for samples of Eph-Pi and Eph-QL, respectively. These components were determined with the best-fitting parameter ranged from 1.00 to 1.1. The range of the experimental errors for the PAL parameters τ_1, τ_2, τ_3, I_1, I_2 and I_3, determined over multiple measurements, were found to be <4 ps, <20 ps, <30 ps, 0.9%, 0.8% and 0.7%, respectively. The mean lifetime of positron was calculated using the following relation

$$\tau_m = (\tau_1 I_1 + \tau_2 I_2 + \tau_3 I_3)/ (I_1 + I_2 + I_3).$$

A free-volume cell model for the positron annihilation was used to explain the observed *o*-Ps lifetimes in molecular solids and polymers [37]. A simple correlation curve was obtained using a rigid spherical potential of radius R with an electron layer of thickness ΔR [38, 39]. Assuming that the annihilation rate of *o*-Ps inside the electron layer is 2 ns^{-1}, which is a spin averaged annihilation rate between *p*-Ps and *o*-Ps, or the annihilation rate of Ps anion [37] the pick-off annihilation lifetime of *o*-Ps, τ_3, in a rigid spherical potential is given by,

$$\tau_3 = 0.5[1-R/R_0+(1/2\pi)\times\sin(2\pi R/R_0)]^{-1}$$

with the units of nm and ns for R and τ_3, respectively, and $R_0 = R + \Delta R$ where ΔR is determined to be 0.166 nm for zeolites and other porous materials [37]. The mean free volume, V_f, can be calculated by a simple relation given below, assuming a spherical shape for the holes [40, 41], $V_f = (4/3)\pi R^3$.

2.5 Biological assessment

2.5.1 Antibacterial activity

The antimicrobial activities of the newly synthesized CT complexes and the pure solvent were tested *in vitro* against two Gram-positive bacteria, *Staphylococcus aureus* and *Bacillus subtilis*, and two Gram-negative bacteria, *Escherichia coli* and *Pseudomonas aeruginosa*, using a modified Bauer–Kirby disc diffusion method [42]. For these investigations, 100 μl test bacteria were grown in 10 ml fresh medium until they reached a count of approximately 10^8 cells/ml for bacteria or 10^5 cells/ml for fungi [43]. Then, 100 μl microbial suspension was spread onto agar plates. The nutrient agar medium for the antibacterial tests consisted of 0.5% peptone, 0.1% beef extract, 0.2% yeast extract, 0.5% NaCl and 1.5% agar-agar [44]. Isolated colonies of each strain were selected from the primary agar plates and tested for susceptibility. After the plates were incubated for 48 h at 37 °C, the inhibition (sterile) zone diameters (including the disc) were measured using slipping calipers from the National Committee for Clinical Laboratory Standards (NCCLS, 1993) [45] and are expressed in mm. The screening was performed using 100 μg/ml CT complex. An antibiotic disc of tetracycline (30 μg/disc, Hi-Media) was used as a positive control.

2.5.2 Antifungal activity

The newly synthesized complexes were also screened for their antifungal properties against *Aspergillus flavus* and *Candida albicans* in DMSO using a modified Bauer–Kirby disc diffusion method [42]. The complexes were dissolved in DMSO. The medium for the antifungal tests consisted of 3% sucrose, 0.3% $NaNO_3$, 0.1% K_2HPO_4, 0.05% KCl, 0.001% $FeSO_4$ and 2% agar-agar [44]. The disc diffusion method for the filamentous fungi was tested using the M38-A standard method [46], whereas the disc diffusion method for yeast was tested using the M44-P standard method [47]. Plates inoculated with filamentous fungi or yeast was incubated for 48 h at 25°C or 30°C, respectively. The antifungal activity of the CT complexes was compared with that of amphotericin B (30 μg/disc, Hi-Media) as a standard antifungal agent. Antifungal activity was determined by measuring the diameters of the sterile zone (mm) in triplicate.

3. RESULTS AND DISCUSSION

3.1 Elemental analyses results

Elemental analyses (CHN) of the Eph-QL and Eph-Pi CT complexes were performed, and the obtained analytical data are as follows:

     1   [(Eph)(QL)]: $C_{16}H_{21}NO_3$; Mol. wt. = 275.34; Calc.: %C, 69.73; %H, 7.63; %N, 5.08, Found: %C, 69.51; %H, 7.47; %N, 5.33

     2   [(Eph)(Pi)$_2$]; $C_{22}H_{19}N_7O_{15}$; Mol. wt. = 621.42; Calc.: %C, 42.52; %H, 3.08; %N, 15.78, Found: %C, 42.31; %H, 2.96; %N, 15.64.

The resulting values are in good agreement with the calculated values, and the suggested values are in agreement with the molar ratios determined from the photometric titration curves. The stoichiometry of the two complexes was found to be 1:1 and 1:2 ratios, based on the obtained data, the formed charge-transfer complexes were formulated as [(Eph)(QL)] and [(Eph)(Pi)$_2$].

3.2 Electronic absorption spectra
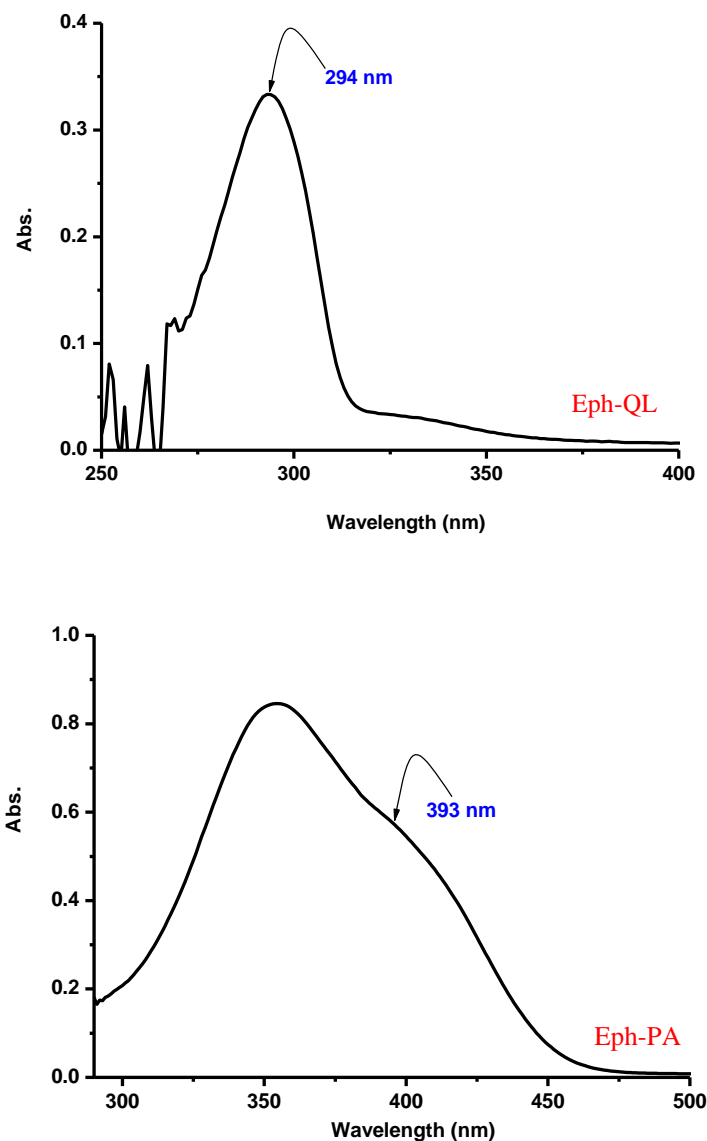
Figure 1. Electronic absorption spectra of Eph-QL (294 nm) and Eph-Pi (393 nm) CT complexes.

Fig. 1 shows the electronic absorption spectra of the formed Eph–QL and Eph–Pi CT complexes. These spectra revealed new absorption bands that are attributed to the CT interactions. These bands are observed at 294 and 393 nm for the [(Eph)(QL)] and [(Eph)(Pi)$_2$] complexes,

respectively. These peak absorbance values that appeared in the spectra assigned to the formed CT complexes were measured and plotted as function of the C_d:C_a ratio according to the known method. Photometric titration plots based on these measurements (Fig. 2) confirmed the complex formation at a ratio (Eph: acceptor) of 1:1 or 1:2.
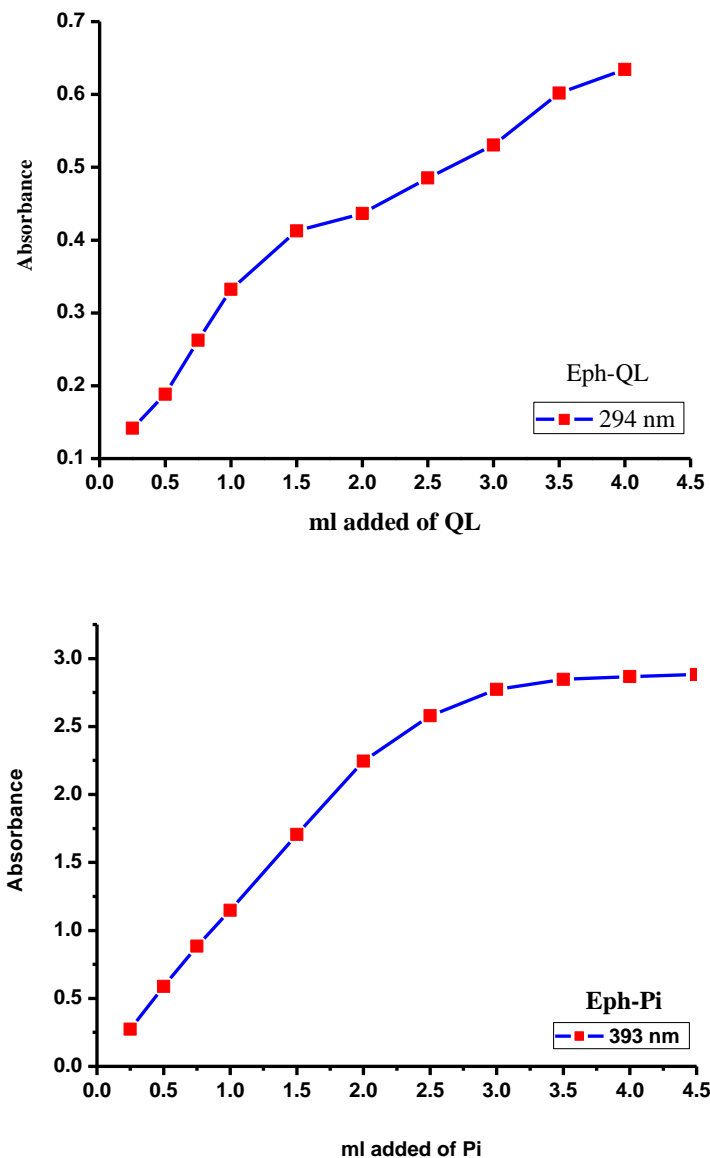
Figure 2. Photometric titration curves for Eph-QL and Eph-Pi CT complexes.

The formation constant (K_{CT}) and the molar absorptivity (ε) of these complexes were calculated by applying the 1:1 and 1:2 modified Benesi–Hildebrand equation in Eqs. (1a, b) [33, 34]:

$$(C_a\, C_d)/A = 1/K\varepsilon + (C_a + C_d)/\varepsilon \quad (1a)$$

where, C_a and C_d are the initial concentrations of the acceptor and the drug donor, respectively, and A is the absorbance of the strongly detected CT band. Plotting $(C_a\,C_d)/A$ values versus the corresponding $(C_a + C_d)$ values for the formed charge-transfer complexes, straight line are obtained supporting our finding of the formation of 1:1 [(Eph)(QL)] complex. In the plots, the slope and intercept equal $1/\varepsilon$ and $1/K\varepsilon$, respectively.
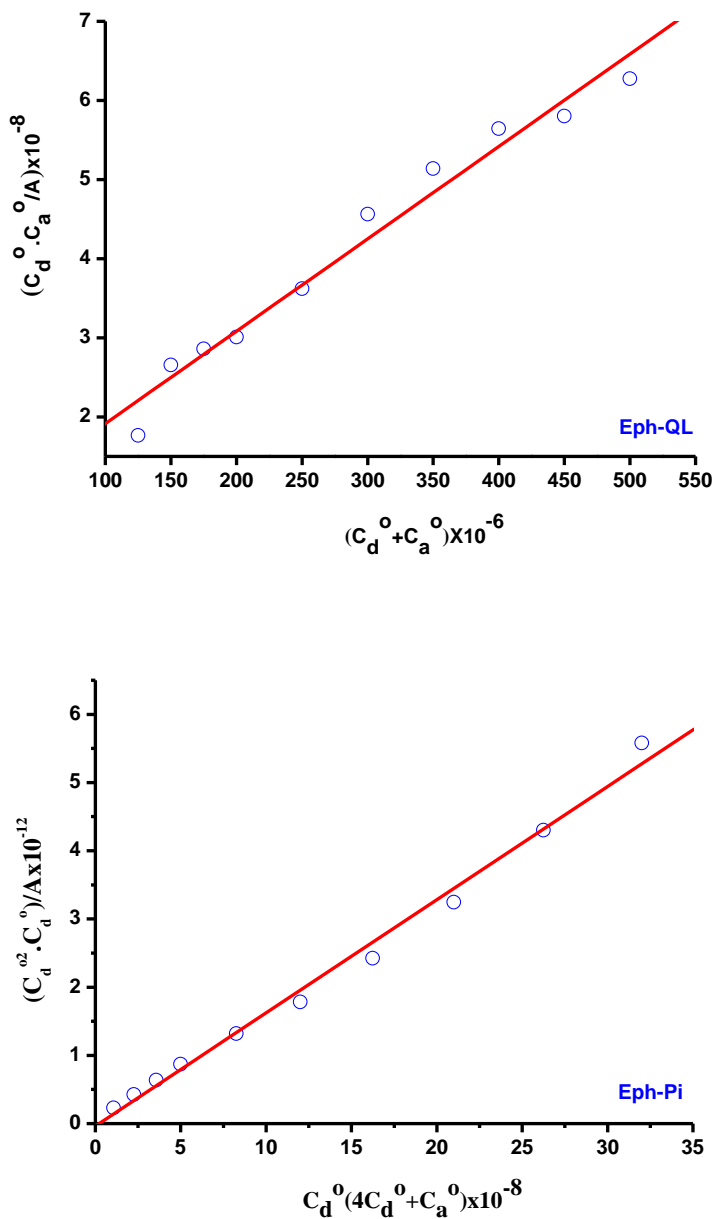
Figure 3. The modified Benesi-Hildebrand plot of Eph-QL and Eph-Pi CT complexes.

The modified Benesi–Hildebrand plots are shown in Fig. 3, and the values of C_d, C_a, $C_d + C_a$ and $C_d . C_d/A$ were calculated. The values of both K_{CT} and ε associated with the 1:1 complex are given in Table 1.

Table 1. Spectrophotometric results of the Eph-QL and Eph-Pi CT complexes

Complex	CT-absorption (nm)	E_{CT} (eV)	K (Lmol^{-1})	ε_{max} (Lmol^{-1}cm^{-1})	f	μ	I_p	R_N	ΔG° (25 °C) (kJmol^{-1})
[(Eph)(QL)]	294	4.320	1.57×10^4	8.56×10^4	12	28	10.96	0.99	-35.346
[(Eph)(Pi)$_2$]	393	3.164	4.47×10^8	6.02×10^4	26	47	9.653	0.662	-49.356

The known equation (1b) for the 1:2 [(Eph)(Pi)$_2$] complex was used in the calculations.

$$(C_a)^2\, C_d/A = 1/K\varepsilon + 1/\varepsilon\, C_a\, (4C_d + C_a) \qquad (1b)$$

where C_d and C_a are the initial concentration of the Pi acceptor and donor (Eph), respectively, and A is the absorbance of the detected CT-band. The data obtained C_d of (Eph), C_a of (Pi), C_a ($4C_d + C_a$) and $(C_a)^2\, C_d/A$ in MeOH were estimated. By plotting $(C_a)^2\, C_d/A$ values vs., C_a ($4C_d + C_a$), straight lines were obtained with a slope of $1/\varepsilon$ and an intercept of $1/K\varepsilon$ as shown in Fig. 2 for the reaction in methanol solvent. The values of both K and ε associated with [(Eph)(Pi)$_2$] complex are given in Table 1. These QL and Pi complexes exhibit high values of both the formation constant (K_{CT}) and the extinction coefficients (ε). These high values of K_{CT} reflect the high stabilities of the formed CT complexes. The data reveal that the [(Eph)(Pi)$_2$] complex shows a higher K_{CT} value compared with the [(Eph)(QL)] complex. This value is four order of magnitude higher than that for the complex [(Eph)(QL)], reflecting the relatively higher powerful electron acceptance ability for nitro groups.

3.3 Calculation of the spectroscopic and physical data

The spectroscopic and physical data, such as the standard free energy ($\Delta G°$), the oscillator strength (f), the transition dipole moment (μ), the resonance energy (R_N), and the ionization potential (I_P), were estimated for samples dissolved in methanol at 25 °C. The calculations can be summarized as follow:

3.3.1 Calculation of oscillator strength (f)

The oscillator strength (f) is a dimensionless quantity used to express the transition probability of the CT-band from the CT absorption spectra [48], and can be estimated using the approximate formula [49]:

$$f = 4.319\times10^{-9} \int \varepsilon_{CT}\, dv \qquad (2)$$

where $\int \varepsilon_{CT}\, dv$ is the area under the curve of the extinction coefficient of the absorption band in question plotted as a function of frequency. To a first approximation,

$$f = 4.319 \times 10^{-9} \, \varepsilon_{CT} \nu_{\frac{1}{2}} \tag{3}$$

where ε_{CT} is the maximum extinction coefficient of the CT band, and $\nu_{\frac{1}{2}}$ is the half-bandwidth in cm^{-1} (i.e., the width of the band at half the maximum extinction).

3.3.2 Calculation of transition dipole moment (μ)

The transition dipole moments (μ) of the CT complexes have been calculated from Eq. (4) [50]:

$$\mu = 0.0958 \, [\varepsilon_{CT} \nu_{\frac{1}{2}} / \nu_{max}]^{\frac{1}{2}} \tag{4}$$

The transition dipole moment can be used to determine if a particular transition is allowed; the transition from a bonding π orbital to an antibonding π^{*} orbital is allowed because the integral that defines the transition dipole moment is non-zero.

3.3.3 Calculation of ionization potential (I_P) of the donor

The ionization potentials (I_P) of the drug donor in the charge-transfer complexes were calculated using the empirical equation derived by Aloisi and Pignataro represented in Eq. (5) [51]:

$$I_P \, (eV) = 5.76 + 1.53 \times 10^{-4} \nu_{CT} \tag{5}$$

where ν_{CT} is the wavenumber in cm^{-1} that corresponds to the CT band formed from the interaction between the donor and the acceptor. The electron-donating power of a donor molecule is measured by its ionization potential, which is the energy required to remove an electron from the highest occupied molecular orbital.

3.3.4 Calculation of resonance energy (R_N)

Briegleb and Czekalla [52] theoretically derived the following relationship to obtain the resonance energy (R_N):

$$\varepsilon_{CT} = 7.7 \times 10^{-4} / \, [h \nu_{CT} / [R_N] - 3.5] \tag{6}$$

where ε_{CT} is the molar absorptivity coefficient of the CT complex at the maximum of the CT absorption, ν_{CT} is the frequency of the CT peak, and R_N is the resonance energy of the complex in the ground state, which contributes to the stability constant of the complex (a ground-state property).

3.3.5 Calculation of energy of the charge-transfer complex (E_{CT})

The energy values (E_{CT}) of the n$\rightarrow$π* and π$-$π* interactions between the donor and the acceptor were calculated using the equation derived by Briegleb [53]:

$$E_{CT} = (h\nu_{CT}) = (1243.667/\lambda_{CT}) \tag{7}$$

where λ_{CT} is the wavelength of the CT band of the formed complex.

3.3.6 Calculation of standard free energy changes ($\Delta G°$)

The standard free energy of complexation ($\Delta G°$) for each complex was calculated from the formation constants using the equation derived by Martin et al. [54]:

$$\Delta G° = -2.303RT \log K_{CT} \tag{8}$$

where $\Delta G°$ is the free energy change of the CT complex (kJmol^{-1}), R is the gas constant (8.314 Jmol^{-1}K), T is the absolute temperature in K, and K_{CT} is the formation constant of the complex (Lmol^{-1}) at room temperature.

The calculated spectroscopic and physical values (f, μ, I_P, R_N and $\Delta G°$) for the obtained CT complexes using these equations are presented in Table 1. [(Eph)(Pi)$_2$] complex exhibits considerably higher values of both the oscillator strength (f) and the transition dipole moment (μ). The observed high values of f indicate a strong interaction between the donor–acceptor pairs with relatively high probabilities of CT transitions [55]. The obtained values of $\Delta G°$ for the [(Eph)(QL)] and [(Eph)(Pi)$_2$] complexes are -35 and -49 kJmol^{-1}, respectively; these negative values indicate that the interaction between the drugs and π–acceptors is exothermic and spontaneous [56, 57].

3.4 IR spectra

Table 2. Characteristic infrared frequencies (cm^{-1}) and tentative assignments of Eph, Pi, QL and their CT complexes

Eph	Pi	QL	[(Eph)(QL)]	[(Eph)(Pi)$_2$]	Assignments[a]
3330	3416	3262	3321	3330	ν(O-H)
2972	-	-	2940	2957	ν(N-H)
-	-	-	2846 2750	2845 2756	Hydrogen bond
1591	-	-	1580	1539	δ(N-H)
1051	1265	1244	1208	1129	ν(C-O)

[a] ν, stretching; ν_s, symmetrical stretching; ν_{as}, asymmetrical stretching; δ, bending.
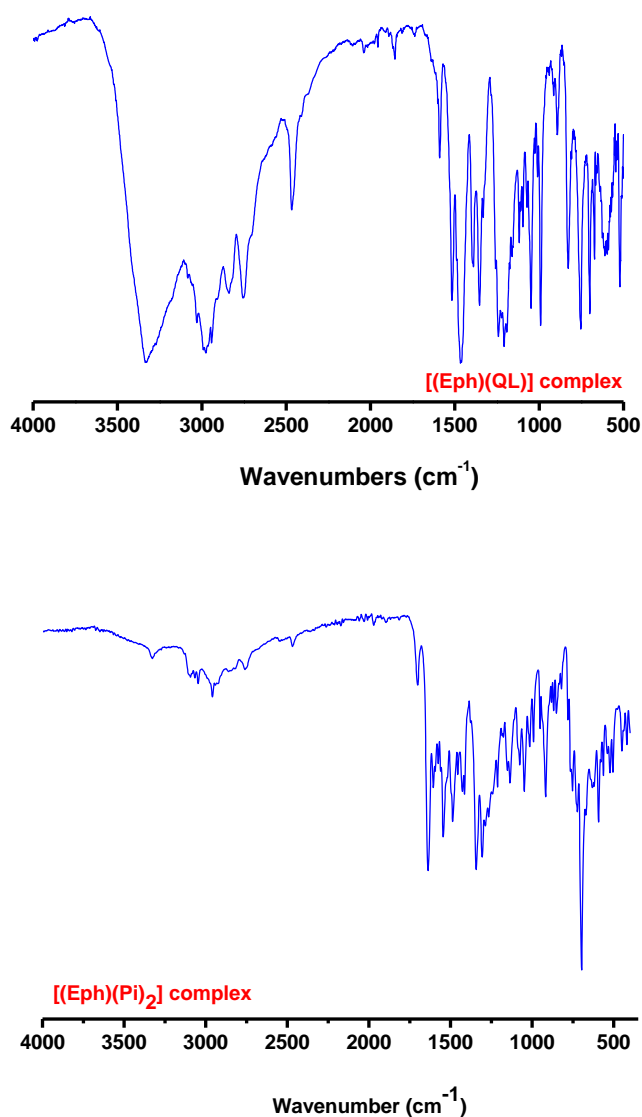
Figure 4. Infrared spectra of Eph-QL and Eph-Pi CT complexes.

The IR absorption spectra of the solid CT complexes were registered in the frequency range 4000-400 cm^{-1} using KBr disc. Their spectra are shown in Fig. 4 while their characteristic band assignments are given in Table 2.

The spectrum of free Eph drug displays a series of significant bands as 3330, 2972 and 1591 cm^{-1} which may assign to $\nu(OH)$, $\nu(NH)$ and $\delta(NH)$. In the IR spectra of the [(Eph)(QL)] and [(Eph)(Pi)$_2$] complex, the characteristic band of Eph observed at 2972 cm^{-1}, which is assigned to $\nu(NH)$ stretching vibration, shifted to lower value and reduced in intensity after complexation. Also, the IR spectrum of this complex is characterized by medium-to-weak bands that appear between 2400-2800 cm^{-1}, which does not appear in the spectrum of the free Eph drug or that of the QL and Pi acceptors. These peaks are due to hydrogen bonding in the complex formed through the transfer of a

proton from QL or Pi to the -NH group of the Eph drug. These observations clearly indicate that the complexation occurs through the protonation of the –NH group in the Eph via a proton-transfer phenomenon from the acidic center of QL and Pi acceptors to the lone pair of electrons on the Eph nitrogen atom based on acid–base theory [58-63]. The IR spectrum of the [(Eph)(Pi)$_2$] complex was recorded distorted in the ν(OH) band, which existed at 3330 cm^{-1}, this may could be interpreted as a result of the formation of intermolecular hydrogen bond between –OH of Eph donor and –OH of the other Pi acceptor molecule. Based on these data, the suggested complexation mechanism between Eph drug with Pi and QL acceptors is illustrated in Scheme I.

3.5 ^{1}H-NMR spectra
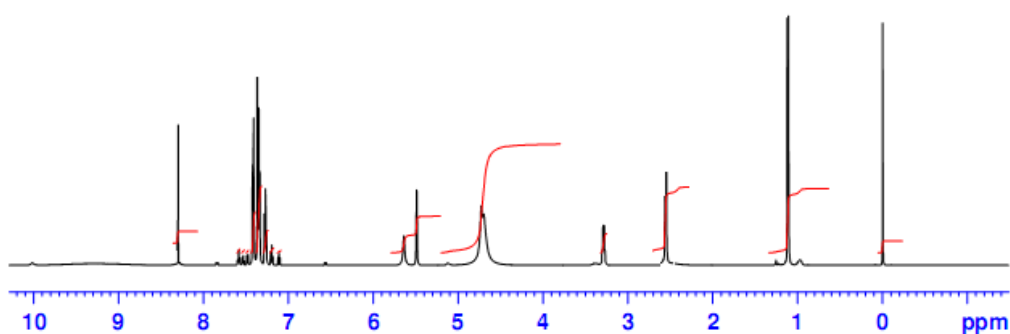
Figure 5a. ^{1}H-NMR spectrum of [(Eph)(QL)] complex.
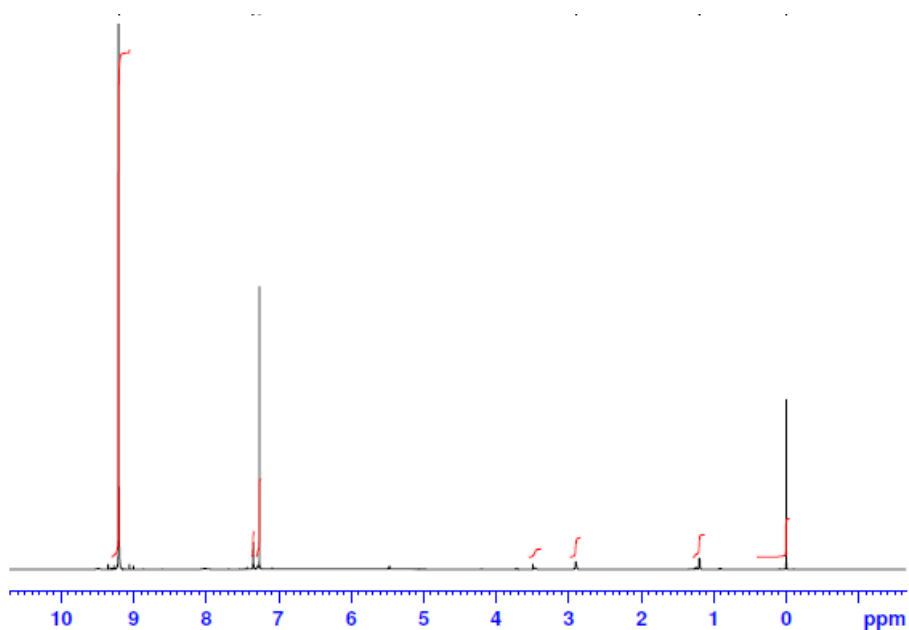
Figure 5b. ^{1}H-NMR spectrum of [(Eph)(Pi)$_2$] complex.

The proton transfer from QL and Pi to the Eph drug was further confirmed by measuring the ^{1}H-NMR spectra of the formed complexes. The 400 MHz nuclear magnetic resonance (^{1}H-NMR)

spectra of the [(Eph)(QL)] and [(Eph)(Pi)$_2$] complex were measured in DMSO-d_6 at room temperature and are given in Fig. 5. The reaction of Eph with QL yielded a new charge-transfer complex, which produced signals at (Fig. 5) [(Eph)(QL)]: δ = 1.11 (s, 3H, CH$_3$), 2.60 (s, 3H, CH$_3$), 3.28 (m, 1H, C$\underline{H}$-CH$_3$), 4.69 (s, 2H, NH$_2^+$ Hydrogen bonded), 5.48 (s, 1H, OH of ephedrine), 5.63 (d, 1H, C$\underline{H}$-OH of ephedrine), 7.10-7.58 (m, 9H, ephedrine and quinol ring protons), 8.30 (s, 1H, quinol phenolic proton). It has been found that, the phenolic proton (–OH) signal, which is observed at δ~8.59 ppm in the spectrum of the free QL acceptor [62], decreased in intensity with an upfield shift for the non-hydrogen-bonded one (δ~8.30) in the spectrum of the CT complex. Instead, a new single peak is observed at 4.69 ppm, which is not detected in the spectrum of the free Eph drug, attributing to two protons of –NH$_2^+$. This situation confirmed the transfer of the phenolic proton of QL to the (-NH) group of Eph. The three signals at 1.11 ppm (3H), 2.60 ppm (3H) and 3.28 ppm (1H), corresponding to the protons of N-CH$_3$, C-CH$_3$ and CH groups, respectively. The [(Eph)(Pi)$_2$] complex produced signals at: δ = 1.192 (s, 3H, CH$_3$), 1.203 (s, 3H, CH$_3$), 2.903 (m, 1H, C$\underline{H}$-CH$_3$), 9.210 (s, 4H, NH$_2^+$ and OH$_2^+$ Hydrogen bonded), 3.500 (s, 1H, C$\underline{H}$-OH of ephedrine), 7.269, 7.351,7.358 (m, 9H, ephedrine and two Pi molecules protons). It has been found that, the phenolic proton (–OH) signal, which is observed at δ~11.0 ppm in the spectrum of the free Pi acceptor absent in the spectrum of the CT complex. Instead, a new single peak is observed at 9.210 ppm, which is not detected in the spectrum of the free Eph drug, attributing to four protons of –NH$_2^+$ and –OH$_2^+$. This situation confirmed the transfer of the phenolic proton from two Pi molecule to both (–NH) and (–OH) groups of Eph drug.

[(Eph)(QL)] complex
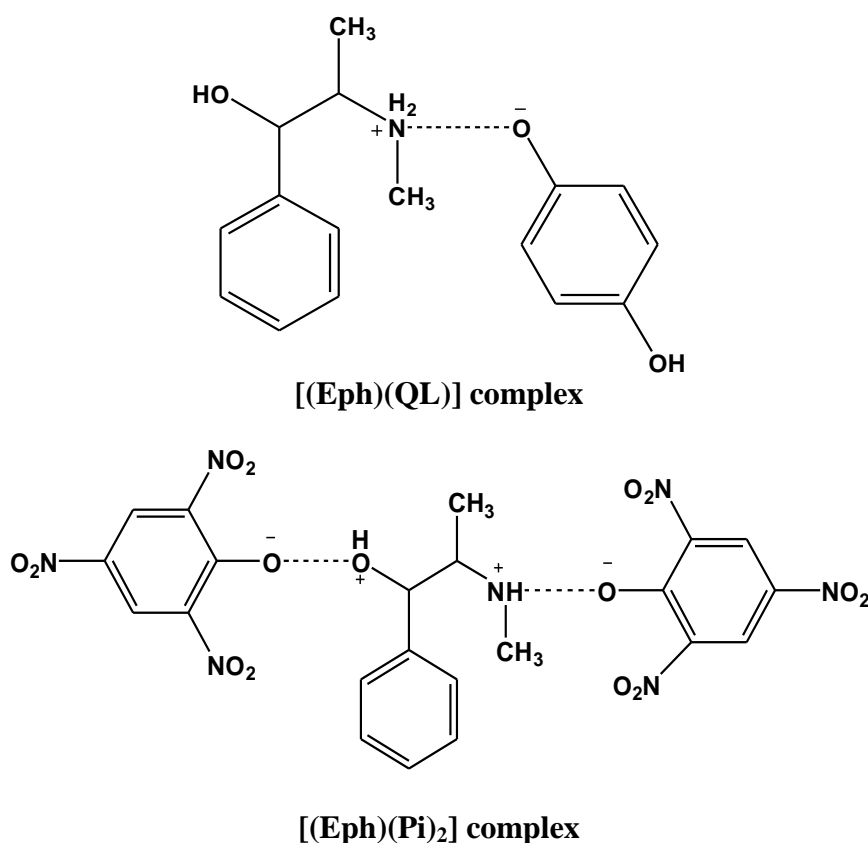
[(Eph)(Pi)$_2$] complex

Scheme I: Complexation mechanism between Eph drug with QL and Pi acceptors

3.6 Thermal analysis
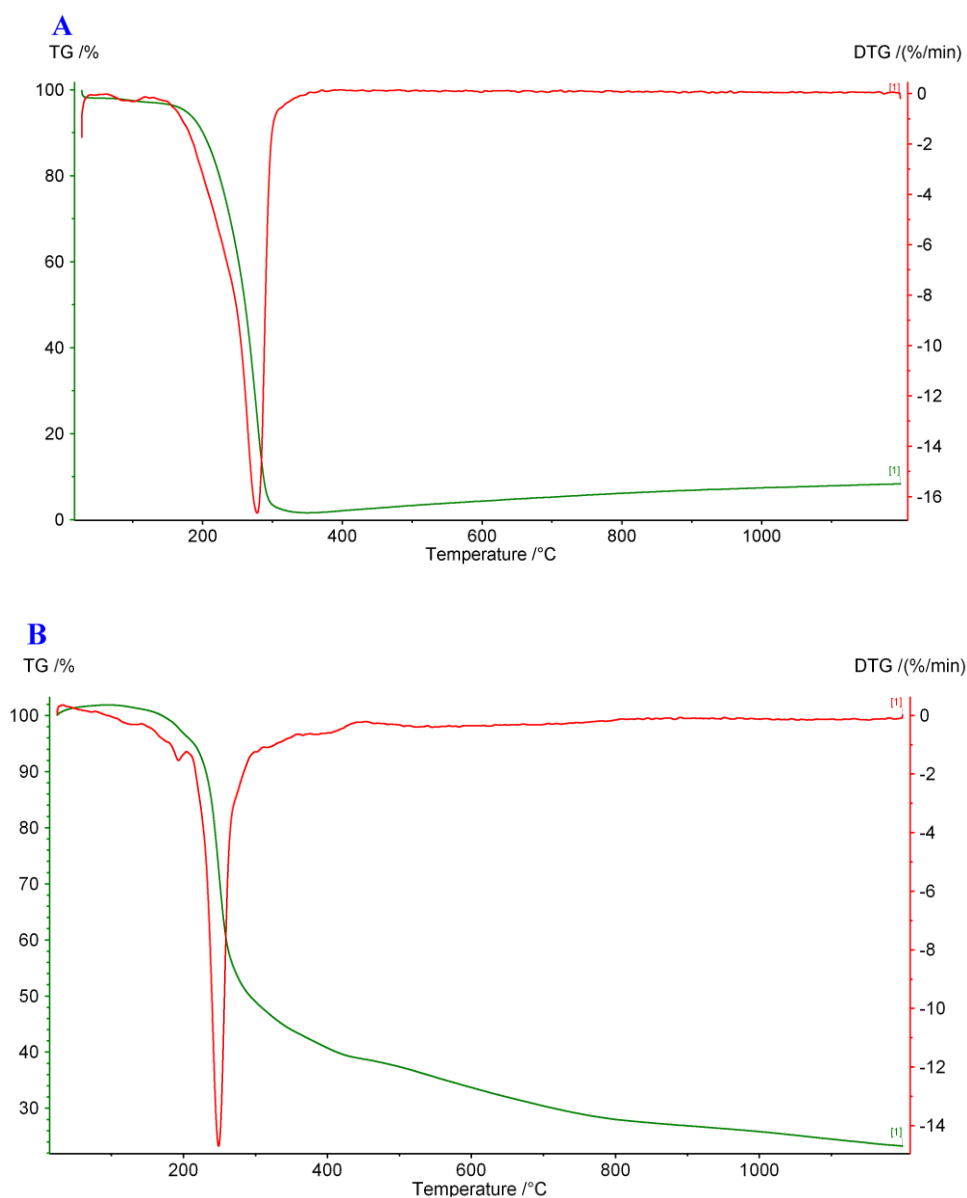
Figure 6. TG/DTG curves of (A) [(Eph)(QL)] and (B) [(Eph)(Pi)$_2$] CT complexes.

Simultaneous thermogravimetric and differential thermogravimetric TG/DTG of the [(Eph)(QL)] and [(Eph)(Pi)$_2$] complexes are shown in Fig. 6. These curves show mass losses in steps, corresponding to endothermic peaks attributed to decomposition of the complexes. In the two TG/DTG curves, the results show good agreement with the calculated formulas as suggested from the analytical data. The curve of [(Eph)(QL)] complex shows mass losses in one main overlapping step between 200 and 1000 °C, corresponding to the very strong endothermic peak at 280 °C, and is assigned to decomposition of two organic moieties; Eph and QL with mass loss of $C_{16}H_{21}NO_3$ ($7C_2H_2+NO_2+2CO_2+3.5H_2$). From TG/DTG curve of [(Eph)(Pi)$_2$] complex, the mass loss that occurs between 160 and 1000 °C, corresponding to the single endothermic peak at 250 °C, is due to the

decomposition of one molecule of Eph drug and two Pi molecules with mass loss 76.74% with 23.26% residual carbons.

3.7 Pharmacology

The obtained CT complexes were screened *in vitro* for their antibacterial and antifungal activity. The complexes to be tested were dissolved in DMSO to obtain 100 μg/ml stock solutions. The diameter zones were measured to determine their effects on the growth of the tested microorganisms.

3.7.1 Antibacterial activity studies
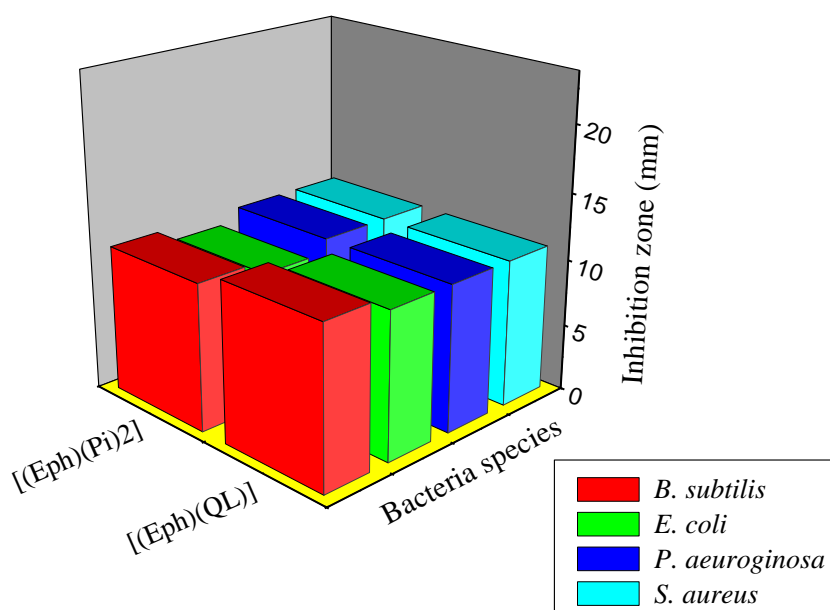
Figure 7. Statistical representation for antibacterial activity of Eph-QL and Eph-Pi CT complexes.

The antibacterial activity of the obtained CT complexes were tested *in vitro* against two Gram-positive bacterial strains, *Staphylococcus aureus* (*S. aureus*) and *Bacillus subtilis*, and two Gram-negative bacterial strains, *Escherichia coli* (*E. coli*) and *Pseudomonas aeruginosa* (*P. aeruginosa*). The activity was determined by measuring the inhibition zone diameter values (mm) of the complexes against the microorganisms. Tetracycline was used as a positive control. The screening data are given in Table 3 and are statistically presented in Fig. 7. The data reveal that the [(Eph)(QL)] and [(Eph)(Pi)$_2$] complexes had exerted moderate inhibitory activity against the growth of the Gram-positive and Gram-negative bacteria species.

Table 3. The inhibition diameter zone values (mm) for [(Eph)(QL)] and [(Eph)(Pi)$_2$] CT complexes

Sample		Inhibition zone diameter (mm/mg sample)					
		Bacteria				Fungi	
		Bacillus subtilis, (G$^+$)[a]	*Escherichia coli,* (G$^-$)	*Pseudomonas aeuroginosa,* (G$^-$)	*Staphylococcus aureus,* (G$^+$)	*Aspergillus flavus*	*Candida albicans*
Control: DMSO		0.0	0.0	0.0	0.0	0.0	0.0
Standard	Tetracycline (Antibacterial agent)	34	32	34	30	-	-
Standard	Amphotericin B (Antifungal agent)	-	-	-	-	18	19
[(Eph)(QL)]		12	11	11	11	0.0	0.0
[(Eph)(Pi)$_2$]		11	10	11	11	0.0	11

[a] G: Gram reaction

3.7.2 Antifungal activity studies
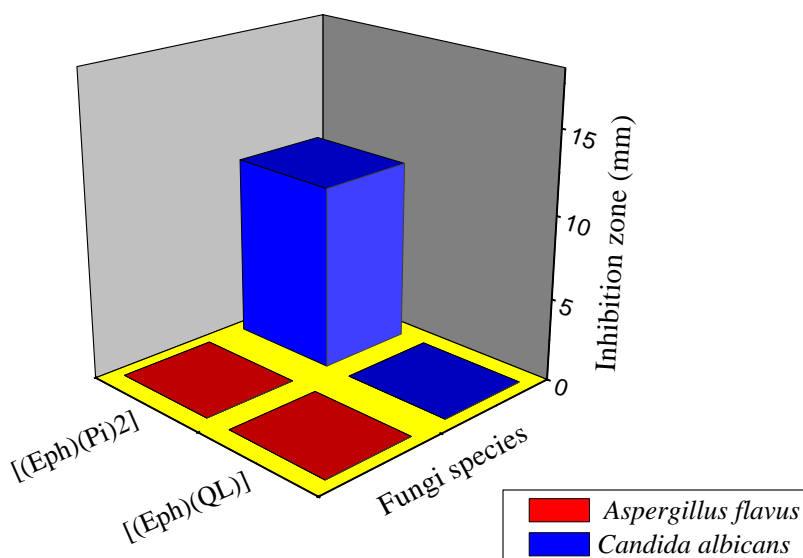
Figure 8**.** Statistical representation for antifungal activity of Eph-QL and Eph-Pi CT complexes.

The synthesized CT complexes were also screened for their antifungal properties against two fungal species, *Aspergillus flavus* and *Candida albicans*. Amphotericin B was used as a positive control, and the screening data are reported in Table 3 and statistically presented in Fig. 8. The results indicated that [(Eph)(Pi)$_2$] complex had a good antifungal response against *Candida albicans*, whereas [(Eph)(QL)] complex exhibited no inhibitory activity against either fungal strains.

3.8 Positron annihilation studies

The lifetime spectra of the Eph-QL complex were decomposed into three components, a short lived (τ_1), an intermediate lived (τ_2) and a longest lived (τ_3). The τ_1 is attributed to the p-Ps and free annihilations. The τ_2 is attributed to the annihilation of positrons or positronium in defect of the ordered structure. The τ_3 is attributed to pick-off annihilation of the o-Ps in the free volume sites present in the CT complex, which is very sensitive to the microstructural changes. Table 4 lists the PAL parameters (τ_1, τ_2, τ_3, I_1, I_2 and I_3) for samples of Eph-QL and Eph-Pi complexes. The relatively poor time resolution (~300 ps) of the used spectrometer makes the decomposition of the shortest-lived lifetime component τ_1 somewhat impossible. The τ_1 and I_1 values ranged from 247 to 287 ps and from 54.5 to 83.3% for Eph-QL and Eph-Pi complexes, respectively. The high τ_1 value of Eph-Pi complex may be due to its higher K_{CT} value compared with the Eph-QL complex that reflecting the relatively higher powerful electron acceptance ability of Eph-Pi. The donor-to-acceptor molar ratio of 1:2 for Eph-Pi complex compared with the ratio (1:1) of Eph-QL complex may be the main reason for the high value of I_1 in the case of Eph-Pi complex as its structure is clustered system.

Table 4. Positron annihilation lifetime components (τ_1, τ_2 and τ_3) and their intensities (I_1, I_2 and I_3) for the studied samples.

Sample type	τ_1 (ps)	I_1 (%)	τ_2 (ps)	I_2 (%)	τ_3 (ps)	I_3 (%)
Eph-QL complex	247	54.5	601	30.3	1107	15.2
Eph-Pi complex	287	83.3	-	-	895	16.7

For Eph-QL complex, the τ_2 lifetime component was observed with value of 601 ps and intensity of 30.3%. This lifetime component with high intensity may be due to liability structure of this complex. The τ_2 lifetime component was disappeared for the Eph-Pi complex due to the complexation mechanism suggested in scheme 1. The results show that the Ps was formed (I_3) with a range of 15.2-16.7 for both studied CT complexes. The Ps formation in both CT complexes with high intensities may be due to their Lewis base that depends on the complex electronic configuration, and the layers between the donor and acceptor. The τ_3 lifetime component ascribed to the annihilation of *o*-Ps indicates that there is one type of vacant. The results indicate that the τ_3 value of Eph-QL CT complex (1107 ps) is larger than that value of Eph-Pi complex (895 ps) by 24%. This is mainly due to the liability structure of the Eph-QL compared with the clustered structure of Eph-Pi as the donor-to-acceptor molar ratio is 1:1 and 1:2 for Eph-QL and Eph-Pi complexes, respectively. The results indicate that the linear correlation between the biological activity of CT complexes and the PAL parameters, especially the short lived component τ_1 and its intensity I_1, was observed and this is consistent with that previously reported [29]. This observed correlation may be due to the increasing of the delocalized electrons as the biological activity is increased secondly, the dependence of the biological activity on the complex molecular weight that already has a strong correlation with the PAL parameters. The variation of the mean lifetime and mean free volume for the Eph-QL and Eph-Pi

complexes is shown in Fig. 9. The results indicated that the mean lifetime and mean free volume for Eph-QL increased by 25 and 90%, respectively, compared with that of Eph-Pi complex due to its liability structure.
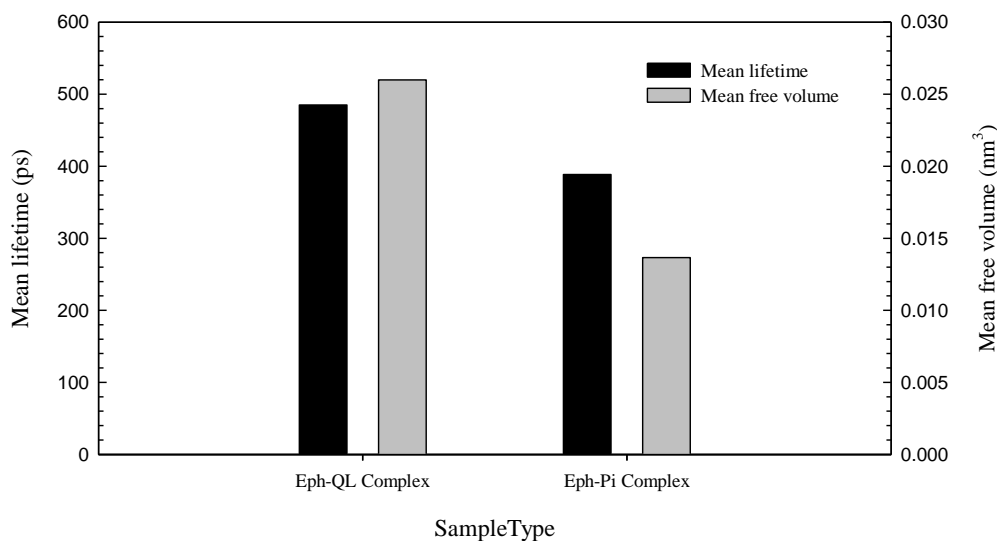
Figure 9. The variation of the mean lifetime (ps) and mean free volume (nm^3) for the studied samples.

4. CONCLUSION

The positron annihilation lifetime parameters were found to be dependent on the properties of the CT complex such as the formation constant, number of layers between the donor and acceptor, donor-to-acceptor molar ratio and ionization potential of the complexes. The molecular weight of the complex affects the mass fraction of the donor component and consequently the fraction of positrons annihilation in that part of the complex. The positron annihilation lifetime components are affected by the biological activity of the CT complex due to the increasing of the delocalized electrons.

References

1. D.K. Roy, A. Saha, A.K. Mukherjee, *Spectrochim. Acta* A 61 (2005) 2017.
2. A.M. Slifkin, Charge-transfer Interaction of Biomolecules, Academic Press, New York, 1971.
3. A. Dozal, H. Keyzer, H.K. Kim, W.W. Wang, Int. J. Antimicrob. Agent 14 (2000) 261.
4. A. Korolkovas, Essentials of Medical Chemistry, 2nd ed., Wiley, New York, 1998 (Chapter 3).
5. F.M. Abou Attia, *Farmaco* 55 (2000) 659.
6. K. Basavaiah, *Farmaco* 59 (2004) 315.

7. G.A. Saleh, H.F. Askal, M.F. Radwan, M.A. Omar*, Talanta* 54 (6) (2001) 1205.

8. H. Salem, *J. Pharm. Biomed. Anal.* 29 (3) (2002) 527.

9. M. Pandeeswaran, E.H. El-Mossalamy, K.P. Elango, *Int. J. Chem. Kinet.* 41 (2009) 787.

10. M. Pandeeswaran, K.P. Elango, *Spectrochim. Acta* A 75 (2010) 1462.

11. M.S. Refat, A.M. El-Didamony, *Spectrochim. Acta* A 65 (3-4) (2006) 732.

12. M.S. Refat, G.G. Mohamed, A. Fathi, *Bull. Korean Chem. Soc.* 31 (6) (2010) 1535.

13. M.S. Refat, S.A. El-Korashy, I.M. El-Deen, S.M. El-Sayed, *J. Mol. Struct.* 980 (2010) 124.

14. M.S. Refat, S.A. El-Korashy, I.M. El-Deen, S.M. El-Sayed, *Drug Test. Anal.* 3 (2011) 116.

15. M.S. Refat, O.B. Ibrahim, H. Al-Didamony, K.M. Abou El-Nour, L. El-Zayat, *J. Saudi Chem. Soc.* 16 (2012) 227.

16. M.S. Refat, *J. Mol. Struct.* 985 (2011) 380.

17. M.S. Refat, W.F. El-Hawary, M.A.A. Moussa, *Spectrochim. Acta* A 78 (2011) 1356.

18. M.S. Refat, A. Elfalaky, E. Elesh, *J. Mol. Struct.* 990 (2011) 217.

19. M.S. Refat, S.A. Sadeek, H.M. Khater, *Spectrochim. Acta* A 64 (3) (2006) 778.

20. M.S. Refat, I. Grabchev, J.-M. Chovelon, G. Ivanova, *Spectrochim. Acta* A 64 (2) (2006) 435.

21. M.S. Refat, H. Al-Didamony, L.A. El-Zayat, *Can. J. Anal. Sci. Spec.* 51 (3) (2006) 147.

22. M.S. Refat, H.M.A. Killa, I. Grabchev, M.Y. El-Sayed, *Spectrochim. Acta* A 68 (1) (2007) 123.

23. M.S. Refat, H.A. Ahmed, Ivo. Grabchev, L.A. El-Zayat, *Spectrochim. Acta* A 70 (4) (2008) 907.

24. M.S. Refat, H.M.A. Killa, I. Grabchev, M.Y. El-Sayed, *Can. J. Anal. Sci. Spec.* 52 (2) (2007) 75.

25. M.S. Refat, L.A. El-Zayat, Okan Zafer Yesilel, *Spectrochimica Acta Part* A 75 (2010) 745.

26. J.C. Machado, G.M. de Lima, F.C. Oliveira, I.M. Marzano, *Chemical Physics Letters* 418 (2006) 292.

27. Marques-Netto, C.F. Carvalho, C.A. Alves de Carvalho, R.D. Sinisterra, H.F. Brito, J.C. Machado, *Chemical Physics Letters* 333 (2001) 371.

28. A.M.A. El-Sayed, H.F.M. Mohamed, A.A.A. Boraei, *Radiation Physics and Chemistry* 58 (2000) 791.

29. Abdelmajid A. Adam, Moamen S. Refat, T. Sharshar, Z.K. Heiba, Spectrochim. Acta Part A, (2012).

30. D.M. Schrader, Y.C. Jean, Studies in Physical and Theoretical Chemistry 57: Positron and Positronium Chemistry; Elsevier; Amsterdam, 1986.

31. W. Brandt, A. Dupasquier (Eds.), Positron solid-state physics. North-Holland; Amsterdam, 1983.

32. D.A. Skoog, Principle of Instrumental Analysis, third ed., Saunders, New York, USA, 1985 (Chapter 7).

33. H.A. Benesi, J.H. Hildebrand, *J. Am. Chem. Soc.* 71 (1949) 2703.

34. R. Abu-Eittah, F. Al-Sugeir, *Can. J. Chem.* 54 (1976) 3705.

35. T. Sharshar, M.L. Hussein, 2005. An optimization of energy window settings for positron annihilation lifetime spectrometers. Nucl. Instr. and Meth. A 546, 584–590.

36. J. Kansy, 1996. Microcomputer program for analysis of positron annihilation lifetime spectra Nucl. Instr. Meth. A 374, 235–244.

37. K. Ito, Y. Ujihira, T. Yamashita, K. Horie, *Journal of Polymer Science* B37 (1999) 2634–2641.

38. S.J. Tao, *J Chem Phys* 56 (1972) 5499.

39. M. Eldrup, D. Lightbody, J.N. Sherwood, *Chem Phys* 63 (1981) 51-58.

40. E.-A. McGonigle, J.J. Liggat, R.A. Pethrick, S.D. Jenkins, J.H. Daly, D. Hayward, *Polymer* 42 (2001) 2413–2426.

41. A.O. Porto, G. Goulart Silva, W.F. Magalhães, *J. Polym. Sci.* 37 (1999) 219–226.

42. A.W. Bauer, W.M. Kirby, C. Sherris, M. Turck, *Am. J. Clin. Pathol.* 45 (1966) 493.

43. M.A. Pfaller, L. Burmeister, M.A. Bartlett, M.G. Rinaldi, *J. Clin. Microbiol.* 26 (1988) 1437.

44. D.J. Beecher, A.C. Wong, *Appl. and Environ. Microbiol.* 60 (1994) 1646.

45. National Committee for Clinical Laboratory Standards. Methods for Antimicrobial Susceptibility Testing of Anaerobic Bacteria: Approved Standard M11-A3. NCCLS, Wayne, PA, USA (1993).

46. National Committee for Clinical Laboratory Standards. Reference Method for Broth Dilution Antifungal Susceptibility Testing of Conidium-Forming Filamentous Fungi: Proposed Standard M38-A. NCCLS, Wayne, PA, USA (2002).
47. National Committee for Clinical Laboratory Standards. Method for Antifungal Disk Diffusion Susceptibility Testing of Yeast: Proposed Guideline M44-P. NCCLS, Wayne, PA, USA (2003).
48. A.B.P. Leve, Inorganic Electronic Spectroscopy, second ed., Elsevier, Amsterdam, 1985, p. 161.
49. H. Tsubomura, R.P. Lang, *J. Am. Chem. Soc*. 83 (1961) 2085.
50. R. Rathore, S.V. Lindeman, J.K. Kochi, *J. Am. Chem. Soc.* 119 (1997) 9393.
51. G. Aloisi, S. Pignataro, *J. Chem. Soc., Faraday Trans*. 69 (1972) 534.
52. G. Aloisi, S. Pignataro, *J. Chem. Soc. Faraday Trans*. 69 (1972) 534.
53. G. Briegleb, *Z. Angew. Chem*. 72 (1960) 401, *Z. Angew. Chem*. 76 (1964) 326.
54. A.N. Martin, J. Swarbrick, A. Cammarata, Physical Pharmacy, 3rd ed., Lee and Febiger, Philadelphia, PA, 1969, p. 344.
55. M.S. Refat, A. Elfalaky, E. Elesh, *J. Mol. Struct.* 990 (2011) 217.
56. K.M. Al-Ahmary, M.M. Habeeb, E.A. Al-Solmy, *J. Mol. Liqs*. 162 (2011) 129.
57. A.S. AL-Attas, M.M. Habeeb, D.S. AL-Raimi, *J. Mol. Struct*. 928 (2009) 158.
58. M.S. Refat, H.A. Saad, A.A. Adam, *J. Mol. Struct.* 995 (2011) 116.
59. L.J. Bellamy, The infrared Spectra of Complex Molecules, Chapman & Hall, London, 1975.
60. R. Bharathikannan, A. Chandramohan, M.A. Kandhaswamy, J. Chandrasekaran, R. Renganathan, V. Kandavelu, *Cryst. Res. Technol*. 43 (6) (2008) 683.
61. A.S. Gaballa, S.M. Teleb, E. Nour, *J. Mol. Struct*. 1024 (2012) 32.
62. A.A. Adam*, J. Mol. Struct*. 1030 (2012) 26.
63. A.A. El-Habeeb, F.A. Al-Saif, M.S. Refat, *J. Mol. Struct*. 1034 (2013) 1.